Supplementary Information

A traceable framework for comparing historic pagoda morphology from 3D heritage meshes

JunLei Zhu and YiFeng Fan

Guide to the supplementary information

This document contains the detailed observations and checks supporting the two architectural comparisons in the article. Tables S1–S3 give eave widths, endpoint coordinates and measurement frames. Tables S4–S9 report comparison and sensitivity results. Tables S10–S11 retain human-review responses and unresolved Liaoyang evidence. Tables S12–S13 identify the working meshes and summarize the calculation. Figure S1 shows sensitivity ranges; Figure S2 shows the exact Chaoyang eave 2 endpoints. The original-photograph context and the eave 2 omission comparison are in main Figures 3 and 5.

Supplementary Note 1 Measurement records and calculation inputs

The case abbreviations are CY, Chaoyang North; CS, Chongshou Temple; QZ, Qingzhou White; CX, Chongxing Temple West; and LY, Liaoyang White. E denotes an eave, numbered upward from the first studied eave. The four main cases are CY, CS, QZ and CX. An asterisk identifies the separate LY conditional analysis, which includes unresolved boundary evidence and does not have the same evidential status as the main comparisons.

Table S1 records 59 eave positions. Forty-six positions belong to the four main cases; 13 belong to LY, but only 12 LY positions have a retained two-direction mean. At LY eave 9, Y′ is retained and X′ is not accepted, so the mean is missing. Table S2 lists 118 raw directional measurements and their 236 endpoint positions. Excluding LY eave 9 X′ leaves 117 directions and 234 endpoints. Thus, the retained profiles contain 58 mean widths, not 59.

Coordinates (x′, y′, z) and widths use local model units. X′ and Y′ are perpendicular horizontal analysis axes, and Z is vertical; the directions are not shared geographic bearings. For X′, subtract the minus endpoint's x′ coordinate from the plus endpoint's x′ coordinate. For Y′, subtract the corresponding y′ coordinates. This is a projected coordinate difference, not the 3D distance between endpoints. The endpoints can have different heights within the same measurement band. The band index starts at one; its lower limit is the grid minimum plus (index − 1) times band thickness, and its upper limit adds one band thickness (Table S3).

A mean width W averages two retained directional widths. Normalized width $w = W/W_1$ divides that mean by the same tower's first studied mean eave width. Relative height h runs from the first studied band center (0) to the last (1), excluding the rest of the tower. A dash means missing, not zero. Raw denotes a geometric candidate before boundary review; adopted, accepted and retained denote measurements used after review. Displayed widths, coordinates and results have at most four decimal places. Small nonzero effects use scientific notation. The underlying full-precision records were not rounded; displayed tables therefore support inspection and approximate recalculation, rather than exact recovery of every numerical tolerance.

Mesh identity, surrounding-geometry masks and coordinate transformations were fixed for each extraction. Table S3 records the source grids; cropping QZ did not reset its 400-band grid. Table S12 identifies the working meshes by SHA256. A matching hash establishes file identity, not the correctness of an architectural boundary or agreement with physical dimensions. Residual model tilt was not independently measured.

Supplementary Note 2 Boundary decisions and their history

Boundary state and source of judgment are different fields. A means the intended architectural boundary was confirmed. B means an unresolved boundary was retained for the separate LY conditional analysis. NA marks a candidate that was not accepted; it contributes no directional width to the adopted mean. Historical inferred geometry, including the LY mirror estimate, is recorded separately and is not substituted for an observation. The retention of B measurements follows

documented assessments at individual locations, rather than a numerical quality threshold. Earlier judgments were carried forward only where the boundary target, coordinates, frame, mask and measurement band corresponded.

The 92 directions in the four main cases have 46 author confirmations, 22 researcher model reviews and 24 inherited model judgments. These counts describe the recorded sources of judgment, not independent reviewers. Fourteen QZ directions trace to the earlier author confirmation of all seven eaves; an intermediate record that called them inherited does not override that source. Table S2 retains the original basis codes so these histories can be distinguished from A/B/NA states.

Chaoyang North eave 2

For CY eave 2 X′, the historical record approved a measurement band before the exact endpoints were subsequently confirmed. The analysis direction also changed from 23° to 22.5°. In a common frame, the positive endpoint moved 2.3763 model units, and the directional width changed from 11.4949 to 11.4370 (−0.5031%). This is a direction-selection change. It is separate from the comparison before and after boundary review, which holds the coordinate frame fixed.

Oblique and plan views were prepared from original triangles within 1.3 model units of each current CY endpoint (Fig. S2). On 10 October 2026 the author confirmed that both points lie on the continuous tile-terminal edge of the same eave, without interference from an ornament, bell or reconstruction artefact. The coordinates were retained. The earlier AI-assisted inspection on 9 October is preserved as historical context and is not counted as independent professional confirmation.

The targeted omission test removes the CY eave 2 mean while retaining the original height limits and first-width denominator. The profile then joins eaves 1 and 3 directly (main Fig. 5). Comparing CY before and after this omission gives $D_1 = 0.0063$, $D_2 = 0.0171$ and $D\infty = 0.0697$. The profiles coincide from eave 3 ($h = 0.1799$) upward. The last-to-first width ratio remains 0.4841; signed residual area changes from −0.0451 to −0.0388. The CY–CS distance decreases by 9.30%, while the quarter-height contrast is unchanged. The first-transition result and the quarter-height result therefore have different dependence on eave 2.

Liaoyang White eave 9

Three LY eave 9 records must be kept distinct. The raw X′ candidate is 16.3250 model units, the historical origin-centered mirror estimate is 16.1898, and the retained Y′ width is 16.1511. The mirror assumes symmetry across the origin and supplies no observed boundary. The targeted review did not confirm the raw X′ boundary, so neither that candidate nor the mirror supplies an adopted X′ value. The raw two-direction mean is 16.2381; the adopted mean is missing. The profile segment between eaves 8 and 10 is interpolation across this missing observation (main Figs. 3 and 7).

The matched comparison before and after review holds meshes, masks, transforms, axes, eave selections and measurement bands fixed. All 117 retained directional widths and all 58 mean widths common to the two calculations are unchanged. Excluding the raw LY eave 9 mean changes the LY profile by $D_1 = 3.84 \times 10^{-4}$, $D_2 = 0.0011$ and $D\infty = 0.0047$. Each of the four between-tower D_1 comparisons involving LY decreases by 3.84×10^{-4}, without changing their ordering (Table S4). These are dependent consequences of one omission. A separate historical-mirror removal scenario reports an L_1 change of 1.07×10^{-4}; it is not the matched raw-versus-adopted calculation.

Human-review records

For the separate human-review exercise, 12 directions were deliberately selected and presented in shuffled order, with earlier grades and study widths hidden. The questions asked whether the endpoints belonged to the intended components, the same eave and the same continuous boundary. Reviewers could answer yes, no or unclear, request additional views or ask for a point to be moved. Circles marked coordinates, not correct answers. Review-item IDs R01–R12 identify directions; reviewer IDs R1 and R2 identify people.

R1 was reported not to have participated in the earlier judgments and to have seen pagodas at sites. The author relayed yes responses for all 12 directions on 12 October 2026. R1 assigned confidence 3/5 to R07 and R12 and 5/5 to the others,

described tile-terminal boundaries without perceived interference, and requested neither point movement nor additional views. No professional background was supplied. Confidence is a reported opinion, not a measure of positional error.

R2 was reported to be a cultural heritage graduate student. The author relayed an unclear response for R07 (LY eave 9 X′). For R12 (LY eave 10 X′), R2 answered yes, retained the point and supplied a marked model plate. The record does not provide a detailed reason for R07, separate reasoning for each endpoint, prior familiarity, the actual review date, confidence or a complete list of registered photographs inspected. The R12 response supports the model interpretation but does not resolve the earlier disputed photograph marker; no verified replacement 3D coordinate was adopted. Eave 10 therefore remains B. The follow-up is a targeted record of judgment, not a representative estimate of reviewer agreement or a final adjudication.

Table S10 preserves the individual responses separately from current measurement use. Table S11 lists all 15 retained B directions. LY eave 9 X′ is a separate unaccepted direction and is not included among those 15. An affirmative response does not automatically resolve a conflict with other evidence or change a measurement's adopted state.

Supplementary Note 3 Numerical procedures and sensitivity tests

These notes expand the tests specified in the main Methods. Profile distances use the sorted union of the two profiles' relative-height positions. On an interval of length Δh with endpoint differences u and v, the squared-difference integral is $\Delta h(u^2 + uv + v^2)/3$. The absolute-difference integral is $\Delta h(|u| + |v|)/2$ when u and v have the same sign or either is zero. If their signs differ, split the interval at the zero crossing and add the two triangular areas. D_1 sums absolute-difference integrals; D_2 is the square root of the summed squared-difference integrals; D_∞ is the largest absolute difference at the combined positions. Residual profiles subtract each tower's own first-to-last straight line before the same calculations.

Each of 48 internal retained mean widths was omitted once. The original first and last heights and first-width denominator were retained, and adjacent remaining observations were joined directly. Each omission affects four between-tower comparisons, giving 192 affected comparisons in total (Table S7; Fig. S1). The separate CY eave 2 result is detailed in Note 2. In band-shift tests, every selected band within a case moves by the same offset of −2, −1, 0, +1 or +2 bands. The original relative heights remain fixed, while the shifted first-band width supplies the denominator. Five choices for each of two cases give 25 combinations per pair and 250 across ten pairs. LY eave 9 remains missing.

First-width-reference tests replace only the denominator with a neighboring-band width, retain other widths and the original heights, and restore w(0) to one. Thickness tests use 0.5, 1 and 2 times the original band thickness at unchanged centers, with each profile normalized by its own first width. Three choices per case give nine combinations for each highlighted pair. Table S8 reports the signed quarter-height difference and the full-profile distance. These ranges describe specified measurement scenarios, not confidence intervals or calibrated measurement uncertainty.

For the fixed CX mesh, Open3D drew 150,000 or 500,000 surface points using seeds 1101–1110. Points were allocated to the recorded height bands, each requiring at least ten sampled points. Thirteen eaves, two directions, two densities and ten seeds gave 520 records, all meeting that requirement. Width loss compares a sample with the full mesh in the same band. Of 260 matched density comparisons, 231 improved at the higher density (Table S9). The largest neighboring-band width change was 5.17%, and the largest local ±1° mean-width change in CX was 0.68%. These results concern repeated representations of one mesh, rather than independent surveys of the building.

Planar convex hulls were calculated from triangles clipped to the same 58 retained paired bands. Their zero-degree projected widths reproduced the finite-band widths within 10^{-7} model units. The tested directions were 0°–89° in 1° steps. A case's direction was held constant across its eaves and varied independently of the other case's direction. Ninety choices per case give 8,100 combinations per pair, 81,000 distances across ten pairs and 5,220 eave-direction values. Area-equivalent diameter uses hull area; Cauchy mean width uses hull perimeter, as defined in main Eq. (6). Each width definition uses its own first-eave denominator and the original heights (Table S5; main Fig. 6). Convex hulls bridge gaps and retain attached geometry, so these alternatives are diagnostics rather than newly reviewed architectural boundaries.

The recorded computational replay ran four analysis programs on unchanged exported observations using Python ≥3.10, NumPy and pandas. It passed 481 baseline checks, 174 hull-diagnostic checks, 332 adoption-effect checks, 22 CY eave 2

omission checks and 140 input-integrity checks. All ten direct and residual comparisons, 5,220 eave-direction values and 81,000 direction-pair distances were reproduced. The largest direction-distance discrepancy was 1.39×10^{-16}. These are previously recorded checks of numerical consistency; editing this document did not perform a new geometry extraction or establish physical measurement accuracy.

The recorded replay environment used Python 3.12.14, NumPy 2.3.5 and pandas 3.0.1. The separate sampling environment lists Open3D 0.19.0, NumPy 2.5.3 and pandas 3.0.5. These records describe different stages and should not be read as a single environment specification. Algorithm S1 summarizes the calculation without relying on the original folder layout. Exact integrity tolerances apply to the full-precision computational records, not to values reconstructed from the rounded tables.

Photographic crops preserve their aspect ratios and contain no generative repair. The revised R12 plate and blue line are author-supplied annotations, not a new coordinate measurement. Context views use a 12° display rotation without a common physical scale; this display rotation differs from the analysis directions in Table S3. Original mesh triangles and recorded endpoint positions are retained.

Table S1 Complete eave observations and normalized profile inputs

CY, CS, QZ, CX and LY are defined in Note 1. Eaves are numbered upward; band indices start at one. h runs from the first studied eave (0) to the last (1). X′ and Y′ widths and their mean W are in local model units; $w = W/W_1$ is dimensionless and uses the same tower's first studied mean width. A denotes a confirmed boundary, B an unresolved boundary retained conditionally, and NA a candidate not accepted after review. X/Y state lists the two directional states in that order. LY* is the separate conditional case. A dash means missing, not zero; LY eave 9 has a Y′ width but no retained mean. Table S3 gives the source grids.

Case	Eave	Band	h	X′ width	Y′ width	Mean W	$w = W/W_1$	X/Y state
CY	1	159	0.0000	14.1718	14.2476	14.2097	1.0000	A/A
CY	2	179	0.1058	11.4370	11.3193	11.3782	0.8007	A/A
CY	3	193	0.1799	11.1054	11.0544	11.0799	0.7797	A/A
CY	4	209	0.2646	10.7411	10.7123	10.7267	0.7549	A/A
CY	5	225	0.3492	10.5301	10.4846	10.5073	0.7394	A/A
CY	6	240	0.4286	10.1266	10.1567	10.1417	0.7137	A/A
CY	7	256	0.5132	9.9494	9.8731	9.9112	0.6975	A/A
CY	8	271	0.5926	9.5077	9.5630	9.5353	0.6710	A/A
CY	9	286	0.6720	9.1935	9.3537	9.2736	0.6526	A/A
CY	10	301	0.7513	8.8594	8.9587	8.9091	0.6270	A/A
CY	11	317	0.8360	8.3324	8.3409	8.3366	0.5867	A/A
CY	12	333	0.9206	7.7100	7.7228	7.7164	0.5430	A/A
CY	13	348	1.0000	6.8763	6.8812	6.8788	0.4841	A/A
CS	1	134	0.0000	13.2162	13.1960	13.2061	1.0000	A/A
CS	2	154	0.0990	13.1116	13.1337	13.1227	0.9937	A/A
CS	3	171	0.1832	12.3933	12.3826	12.3880	0.9380	A/A
CS	4	188	0.2673	11.7261	11.7040	11.7151	0.8871	A/A
CS	5	205	0.3515	11.1611	11.0744	11.1178	0.8419	A/A
CS	6	221	0.4307	10.3755	10.2555	10.3155	0.7811	A/A
CS	7	237	0.5099	10.0412	9.9816	10.0114	0.7581	A/A
CS	8	254	0.5941	9.4373	9.4842	9.4608	0.7164	A/A
CS	9	271	0.6782	8.9356	8.9592	8.9474	0.6775	A/A
CS	10	287	0.7574	8.3352	8.2902	8.3127	0.6295	A/A
CS	11	303	0.8366	7.6266	7.6117	7.6191	0.5769	A/A
CS	12	322	0.9307	7.1579	7.0748	7.1164	0.5389	A/A

Case	Eave	Band	h	X′ width	Y′ width	Mean W	w = W/W₁	X/Y state
CS	13	336	1.0000	6.4854	6.4355	6.4604	0.4892	A/A
QZ	1	78	0.0000	24.0775	24.0805	24.0790	1.0000	A/A
QZ	2	119	0.1822	22.4394	22.2815	22.3605	0.9286	A/A
QZ	3	158	0.3556	21.3108	21.2777	21.2943	0.8843	A/A
QZ	4	196	0.5244	19.8496	19.9726	19.9111	0.8269	A/A
QZ	5	233	0.6889	18.5780	18.7121	18.6450	0.7743	A/A
QZ	6	268	0.8444	17.6994	17.7187	17.7091	0.7355	A/A
QZ	7	303	1.0000	16.5839	16.4396	16.5117	0.6857	A/A
CX	1	150	0.0000	12.9237	12.9556	12.9397	1.0000	A/A
CX	2	166	0.1119	11.5363	11.4546	11.4955	0.8884	A/A
CX	3	178	0.1958	11.3825	11.2660	11.3243	0.8752	A/A
CX	4	190	0.2797	11.2544	11.0718	11.1631	0.8627	A/A
CX	5	202	0.3636	10.9717	10.7808	10.8762	0.8405	A/A
CX	6	213	0.4406	10.6774	10.4696	10.5735	0.8171	A/A
CX	7	225	0.5245	10.4680	10.1868	10.3274	0.7981	A/A
CX	8	236	0.6014	10.1950	9.9452	10.0701	0.7782	A/A
CX	9	248	0.6853	9.8926	9.6029	9.7477	0.7533	A/A
CX	10	259	0.7622	9.6137	9.3992	9.5064	0.7347	A/A
CX	11	271	0.8462	9.3535	9.1129	9.2332	0.7136	A/A
CX	12	282	0.9231	9.0819	8.9958	9.0388	0.6985	A/A
CX	13	293	1.0000	8.7378	8.5924	8.6651	0.6697	A/A
LY*	1	160	0.0000	20.0101	20.0172	20.0137	1.0000	A/A
LY*	2	172	0.0938	18.3631	18.4036	18.3834	0.9185	B/B
LY*	3	183	0.1797	18.0412	17.9640	18.0026	0.8995	A/A
LY*	4	193	0.2578	17.7268	17.6215	17.6742	0.8831	B/B
LY*	5	204	0.3438	17.4151	17.4354	17.4253	0.8707	A/A
LY*	6	215	0.4297	17.1137	17.1067	17.1102	0.8549	A/A
LY*	7	225	0.5078	16.8215	16.8354	16.8284	0.8408	B/B
LY*	8	235	0.5859	16.4516	16.4693	16.4604	0.8225	B/B
LY*	9	246	0.6719	—	16.1511	—	—	NA/A
LY*	10	256	0.7500	15.8412	15.8727	15.8570	0.7923	B/B
LY*	11	266	0.8281	15.5139	15.5770	15.5454	0.7767	B/B
LY*	12	277	0.9141	15.1114	15.1827	15.1470	0.7568	B/B
LY*	13	288	1.0000	14.9978	14.9177	14.9578	0.7474	B/A

Table S2 Complete signed endpoints and review provenance

Each row is one directional measurement; the case and eave number link it to Table S1. Coordinates (x′, y′, z) are local mode1 units. Minus and plus identify the minimum and maximum coordinates along the stated axis; endpoint heights may differ within the band. Raw width is their projected difference before review. State gives A, B or NA as defined in Note 2. Basis retains historical source codes: U, author confirmation; R, researcher model review; I, inherited judgment; and L, the code used for LY source records. These source codes are separate from boundary states. NA identifies the unaccepted LY eave 9 X′ record. The 15 B directions are explained in Table S11. Retaining equal raw and reviewed widths does not establish agreement with physical dimensions.

Case	Eave and axis	Minus (x′, y′, z)	Plus (x′, y′, z)	Raw width	State	Source
CY	E1 X′	(-6.9522, -5.9479, 16.9058)	(7.2196, -6.3771, 17.0128)	14.1718	A	U
CY	E1 Y′	(6.1793, -7.0819, 17.0128)	(-6.4220, 7.1658, 17.0128)	14.2476	A	U
CY	E2 X′	(-5.5270, 2.8056, 19.1333)	(5.9100, -1.9813, 19.1225)	11.4370	A	U
CY	E2 Y′	(-5.3302, -5.6994, 19.0597)	(1.5757, 5.6199, 19.1528)	11.3193	A	U
CY	E3 X′	(-5.4419, -3.3699, 20.6508)	(5.6635, -5.4623, 20.6065)	11.1054	A	R
CY	E3 Y′	(-3.7701, -5.6594, 20.6508)	(0.1961, 5.3950, 20.5438)	11.0544	A	R
CY	E4 X′	(-5.2736, -5.0231, 22.3628)	(5.4675, -5.3638, 22.3474)	10.7411	A	R
CY	E4 Y′	(-4.8659, -5.5132, 22.3628)	(0.2081, 5.1991, 22.2558)	10.7123	A	R
CY	E5 X′	(-5.1547, -3.7091, 24.0748)	(5.3754, -5.2789, 24.0654)	10.5301	A	R
CY	E5 Y′	(-2.2210, -5.4053, 24.0748)	(0.2306, 5.0792, 23.9678)	10.4846	A	R
CY	E6 X′	(-4.9571, -5.1885, 25.6797)	(5.1695, -5.1267, 25.6172)	10.1266	A	R
CY	E6 Y′	(-0.9002, -5.3024, 25.6797)	(-4.8459, 4.8543, 25.5727)	10.1567	A	R
CY	E7 X′	(-4.8633, -2.4999, 27.3917)	(5.0861, -4.6704, 27.3917)	9.9494	A	R
CY	E7 Y′	(-3.4965, -5.2039, 27.3917)	(-4.6984, 4.6692, 27.2847)	9.8731	A	R
CY	E8 X′	(-4.6607, -1.8314, 28.9967)	(4.8469, -4.2274, 28.9967)	9.5077	A	R
CY	E8 Y′	(-1.8395, -5.0302, 28.9967)	(-4.5312, 4.5328, 28.9362)	9.5630	A	R

Case	Eave and axis	Minus (x′, y′, z)	Plus (x′, y′, z)	Raw width	State	Source
CY	E9 X′	(-4.5822, -4.1174, 30.6017)	(4.6113, -4.6700, 30.5389)	9.1935	A	R
CY	E9 Y′	(-4.1490, -4.9512, 30.6017)	(-4.4245, 4.4025, 30.5606)	9.3537	A	R
CY	E10 X′	(-4.4479, -3.7557, 32.2067)	(4.4115, -3.9413, 32.2067)	8.8594	A	U
CY	E10 Y′	(-3.9984, -4.8175, 32.2067)	(-4.1976, 4.1412, 32.2067)	8.9587	A	U
CY	E11 X′	(-4.1764, -3.8538, 33.9187)	(4.1560, -3.8195, 33.9187)	8.3324	A	R
CY	E11 Y′	(-2.8645, -4.5535, 33.9187)	(-3.9404, 3.7874, 33.8489)	8.3409	A	R
CY	E12 X′	(-3.9269, -3.1658, 35.6306)	(3.7831, -2.8765, 35.6306)	7.7100	A	R
CY	E12 Y′	(-3.4570, -4.2297, 35.6256)	(-3.3775, 3.4931, 35.6306)	7.7228	A	R
CY	E13 X′	(-3.5157, -2.8835, 37.2228)	(3.3606, 2.8884, 37.1286)	6.8763	A	R
CY	E13 Y′	(-1.6699, -3.8476, 37.1927)	(-3.4517, 3.0336, 37.2127)	6.8812	A	R
CS	E1 X′	(-6.5659, 2.6906, 15.3681)	(6.6503, 2.5980, 15.4348)	13.2162	A	I
CS	E1 Y′	(2.7093, -6.5938, 15.4348)	(-2.5208, 6.6023, 15.3322)	13.1960	A	I
CS	E2 X′	(-6.5133, -2.5446, 17.7292)	(6.5983, 2.5720, 17.6674)	13.1116	A	I
CS	E2 Y′	(-2.5599, -6.5636, 17.7194)	(-2.5252, 6.5700, 17.6351)	13.1337	A	I
CS	E3 X′	(-6.1246, -2.3873, 19.6210)	(6.2687, 2.4230, 19.5961)	12.3933	A	I
CS	E3 Y′	(-2.4220, -6.1769, 19.6618)	(-2.4152, 6.2058, 19.6157)	12.3826	A	I
CS	E4 X′	(-5.7780, -2.2618, 21.6229)	(5.9481, 2.2822, 21.6485)	11.7261	A	I
CS	E4 Y′	(-2.3039, -5.8852, 21.6459)	(-2.2701, 5.8188, 21.6435)	11.7040	A	I
CS	E5 X′	(-5.5226, -2.2076, 23.5133)	(5.6385, 2.1747, 23.5148)	11.1611	A	I

Case	Eave and axis	Minus (x′, y′, z)	Plus (x′, y′, z)	Raw width	State	Source
CS	E5 Y′	(-2.1840, -5.5419, 23.5549)	(2.3096, 5.5325, 23.5112)	11.0744	A	I
CS	E6 X′	(-5.1346, -2.0534, 25.3496)	(5.2410, 2.0126, 25.3461)	10.3755	A	I
CS	E6 Y′	(-2.0443, -5.1383, 25.4171)	(2.1218, 5.1172, 25.3700)	10.2555	A	I
CS	E7 X′	(-4.9356, -1.3219, 27.1905)	(5.1056, -2.0411, 27.2275)	10.0412	A	I
CS	E7 Y′	(1.9842, -4.9691, 27.2989)	(1.9994, 5.0124, 27.2989)	9.9816	A	R
CS	E8 X′	(-4.6382, -1.9322, 29.1794)	(4.7991, -1.8834, 29.2404)	9.4373	A	I
CS	E8 Y′	(1.8711, -4.7023, 29.2246)	(1.8692, 4.7820, 29.2448)	9.4842	A	I
CS	E9 X′	(-4.3884, 1.7201, 31.1199)	(4.5472, -1.7217, 31.1761)	8.9356	A	I
CS	E9 Y′	(-1.6494, -4.4565, 31.1097)	(1.6676, 4.5027, 31.1114)	8.9592	A	I
CS	E10 X′	(-4.0637, 1.6134, 32.9916)	(4.2715, 1.8031, 32.9903)	8.3352	A	I
CS	E10 Y′	(-1.4840, -4.1210, 32.9992)	(1.5115, 4.1692, 32.9635)	8.2902	A	I
CS	E11 X′	(-3.7391, 1.3963, 34.8807)	(3.8875, -1.3913, 34.8708)	7.6266	A	I
CS	E11 Y′	(-1.3783, -3.7833, 34.8838)	(1.3415, 3.8284, 34.8430)	7.6117	A	I
CS	E12 X′	(-3.4980, 1.2565, 36.9745)	(3.6599, -1.3926, 37.0383)	7.1579	A	I
CS	E12 Y′	(-1.2791, -3.5757, 37.0684)	(1.2449, 3.4991, 36.9745)	7.0748	A	R
CS	E13 X′	(-3.2208, 1.0753, 38.6803)	(3.2646, -0.8483, 38.6320)	6.4854	A	I
CS	E13 Y′	(-1.2596, -3.2735, 38.7023)	(-1.3500, 3.1619, 38.6350)	6.4355	A	I
QZ	E1 X′	(-11.9509, -5.0825, 14.0506)	(12.1266, -5.0721, 14.0506)	24.0775	A	U
QZ	E1 Y′	(-5.0260, -12.1548, 14.0506)	(5.0670, 11.9257, 14.0506)	24.0805	A	U

Case	Eave and axis	Minus (x′, y′, z)	Plus (x′, y′, z)	Raw width	State	Source
QZ	E2 X′	(-11.1430, -4.6162, 21.5321)	(11.2965, 4.4773, 21.5321)	22.4394	A	U
QZ	E2 Y′	(4.6247, -11.2833, 21.5321)	(4.7186, 10.9982, 21.5321)	22.2815	A	U
QZ	E3 X′	(-10.5177, -4.4459, 28.6993)	(10.7931, 4.2654, 28.6579)	21.3108	A	U
QZ	E3 Y′	(4.4421, -10.7518, 28.6682)	(4.5265, 10.5259, 28.7050)	21.2777	A	U
QZ	E4 X′	(-9.7622, 3.9000, 35.5977)	(10.0875, 3.9942, 35.6664)	19.8496	A	U
QZ	E4 Y′	(4.3825, -10.0754, 35.6143)	(4.0894, 9.8972, 35.5939)	19.9726	A	U
QZ	E5 X′	(-9.1918, -4.0381, 42.3342)	(9.3862, -3.9762, 42.3342)	18.5780	A	U
QZ	E5 Y′	(3.9863, -9.4535, 42.3661)	(3.8509, 9.2586, 42.3342)	18.7121	A	U
QZ	E6 X′	(-8.7410, -3.7410, 48.7460)	(8.9583, -3.6971, 48.7581)	17.6994	A	U
QZ	E6 Y′	(-3.5209, -8.9220, 48.7694)	(3.5797, 8.7967, 48.7209)	17.7187	A	U
QZ	E7 X′	(-8.1316, 3.0751, 55.1075)	(8.4523, -3.2999, 55.1657)	16.5839	A	U
QZ	E7 Y′	(-3.2739, -8.3123, 55.1075)	(-3.2617, 8.1273, 55.1454)	16.4396	A	U
CX	E1 X′	(-6.6064, -2.7368, 16.3032)	(6.3173, -2.6140, 16.2745)	12.9237	A	U
CX	E1 Y′	(2.5414, -6.5069, 16.2690)	(2.3654, 6.4487, 16.2186)	12.9556	A	U
CX	E2 X′	(-5.8791, 2.1410, 17.9657)	(5.6572, -2.3143, 18.0362)	11.5363	A	U
CX	E2 Y′	(2.2583, -5.7321, 18.0752)	(2.0846, 5.7225, 17.9997)	11.4546	A	U
CX	E3 X′	(-5.8450, 2.1371, 19.3156)	(5.5375, -2.2773, 19.3633)	11.3825	A	U
CX	E3 Y′	(2.2385, -5.5866, 19.3948)	(2.0786, 5.6794, 19.3018)	11.2660	A	U
CX	E4 X′	(-5.7838, 2.1108, 20.6227)	(5.4706, -2.1971, 20.6289)	11.2544	A	U

Case	Eave and axis	Minus (x′, y′, z)	Plus (x′, y′, z)	Raw width	State	Source
CX	E4 Y′	(2.2222, -5.4736, 20.7150)	(2.0462, 5.5982, 20.6486)	11.0718	A	U
CX	E5 X′	(-5.6189, 2.0811, 21.9249)	(5.3528, -2.1527, 21.9474)	10.9717	A	U
CX	E5 Y′	(2.1401, -5.3895, 21.9728)	(1.9881, 5.3913, 21.9249)	10.7808	A	U
CX	E6 X′	(-5.4855, 2.0634, 23.1349)	(5.1918, -2.0474, 23.2160)	10.6774	A	U
CX	E6 Y′	(2.0933, -5.1875, 23.2448)	(1.9609, 5.2821, 23.1582)	10.4696	A	U
CX	E7 X′	(-5.4196, 2.0855, 24.4645)	(5.0484, -2.0206, 24.4548)	10.4680	A	U
CX	E7 Y′	(2.0615, -5.0768, 24.4966)	(1.9119, 5.1099, 24.4548)	10.1868	A	U
CX	E8 X′	(-5.2238, 1.9856, 25.7690)	(4.9712, -1.9902, 25.7194)	10.1950	A	U
CX	E8 Y′	(2.0129, -4.9417, 25.7329)	(1.9004, 5.0035, 25.6647)	9.9452	A	U
CX	E9 X′	(-5.1019, 1.9586, 27.0053)	(4.7906, -1.9224, 26.9846)	9.8926	A	U
CX	E9 Y′	(1.8962, -4.7765, 27.0213)	(-2.1777, 4.8265, 26.9846)	9.6029	A	U
CX	E10 X′	(-5.0042, 1.9240, 28.2540)	(4.6095, -1.8307, 28.2525)	9.6137	A	U
CX	E10 Y′	(1.8300, -4.6679, 28.2413)	(1.7945, 4.7313, 28.1945)	9.3992	A	U
CX	E11 X′	(-4.8301, 1.8446, 29.5145)	(4.5234, -1.7985, 29.5145)	9.3535	A	U
CX	E11 Y′	(1.7918, -4.5203, 29.5145)	(1.7416, 4.5926, 29.5145)	9.1129	A	U
CX	E12 X′	(-4.6730, 1.7614, 30.7462)	(4.4089, -1.7367, 30.7823)	9.0819	A	U
CX	E12 Y′	(-1.9272, -4.4069, 30.8124)	(1.7083, 4.5889, 30.7299)	8.9958	A	U
CX	E13 X′	(-4.5242, 1.7313, 31.9831)	(4.2136, -1.7244, 31.9517)	8.7378	A	U
CX	E13 Y′	(1.7044, -4.2376, 32.0397)	(1.6541, 4.3548, 31.9355)	8.5924	A	U

Case	Eave and axis	Minus (x′, y′, z)	Plus (x′, y′, z)	Raw width	State	Source
LY	E1 X′	(-10.0316, 3.6166, 28.0666)	(9.9784, 4.2923, 28.0657)	20.0101	A	L
LY	E1 Y′	(-4.1317, -10.0344, 27.9968)	(2.2953, 9.9828, 27.9840)	20.0172	A	L
LY	E2 X′	(-9.2347, 3.7612, 30.1708)	(9.1284, 3.8686, 30.2414)	18.3631	B	L
LY	E2 Y′	(-3.7504, -9.1694, 30.2132)	(3.6857, 9.2343, 30.2029)	18.4036	B	L
LY	E3 X′	(-9.0657, 3.6836, 32.0935)	(8.9755, -3.6060, 32.1094)	18.0412	A	L
LY	E3 Y′	(-3.6992, -8.9527, 32.1364)	(3.5981, 9.0113, 32.1266)	17.9640	A	L
LY	E4 X′	(-8.9180, 3.5700, 33.9135)	(8.8089, 3.7379, 33.9680)	17.7268	B	L
LY	E4 Y′	(-3.6178, -8.7621, 33.9680)	(-3.6887, 8.8594, 33.9215)	17.6215	B	L
LY	E5 X′	(-8.7607, 3.5820, 35.8359)	(8.6543, 3.7060, 35.8995)	17.4151	A	L
LY	E5 Y′	(-3.6333, -8.6772, 35.9020)	(3.4643, 8.7583, 35.8835)	17.4354	A	L
LY	E6 X′	(-8.5799, 3.4967, 37.6908)	(8.5338, -3.4437, 37.7498)	17.1137	A	L
LY	E6 Y′	(-3.5265, -8.5041, 37.6750)	(3.4146, 8.6026, 37.6640)	17.1067	A	L
LY	E7 X′	(-8.4485, 3.4446, 39.4858)	(8.3731, 3.6015, 39.5090)	16.8215	B	L
LY	E7 Y′	(-3.4785, -8.3757, 39.5248)	(3.3265, 8.4596, 39.4704)	16.8354	B	L
LY	E8 X′	(-8.2552, -3.3849, 41.3453)	(8.1964, -3.2576, 41.3443)	16.4516	B	L
LY	E8 Y′	(-3.3693, -8.1794, 41.3600)	(3.2863, 8.2900, 41.2742)	16.4693	B	L
LY	E9 X′	(-8.0949, -1.0944, 43.1354)	(8.2301, 2.3136, 43.2670)	16.3250	NA	NA
LY	E9 Y′	(2.9562, -8.0241, 43.2271)	(2.9300, 8.1270, 43.1723)	16.1511	A	L
LY	E10 X′	(-7.9752, 2.8517, 44.9726)	(7.8660, 2.3105, 44.9815)	15.8412	B	L

Case	Eave and axis	Minus (x′, y′, z)	Plus (x′, y′, z)	Raw width	State	Source
LY	E10 Y′	(2.7568, -7.9160, 44.9749)	(3.1451, 7.9567, 44.8881)	15.8727	B	L
LY	E11 X′	(-7.7561, 1.8308, 46.7825)	(7.7577, 2.3050, 46.8160)	15.5139	B	L
LY	E11 Y′	(3.1108, -7.7368, 46.8160)	(3.0849, 7.8401, 46.7467)	15.5770	B	L
LY	E12 X′	(-7.5826, -3.0649, 48.6378)	(7.5287, 3.0724, 48.7277)	15.1114	B	L
LY	E12 Y′	(2.6795, -7.5244, 48.7520)	(-3.0960, 7.6583, 48.6147)	15.1827	B	L
LY	E13 X′	(-7.5262, -2.5988, 50.5643)	(7.4716, -0.1013, 50.5409)	14.9978	B	L
LY	E13 Y′	(-2.7058, -7.4392, 50.5780)	(-0.2022, 7.4785, 50.5400)	14.9177	A	L

Table S3 Frozen grids and coordinate transformations

Each source grid has 400 bands. Grid limits and band thickness are in local model units. Band limits use the one-based index in Table S1. The QZ crop retains its original grid. The preparation column records axis mapping, vertical translation and horizontal rotation; these establish local analysis directions, not geographic bearings. The 12° figure-display rotation is separate. Very small reported grid minima reflect numerical roundoff.

Case	Grid Z min	Grid Z max	Thickness	Bands E1–last	Frame and preparation
CY	0.0000	42.7996	0.1070	159–348	(X, −Z, Y); Z minimum removed; yaw +22.5°
CS	0.0000	46.0741	0.1152	134–336	Cropped source; (X, −Z, Y); Z minimum removed; yaw −4.5°
QZ	0.0000	72.9901	0.1825	78–303	Frozen Z-up cropped roof-band mesh; source grid retained
CX	-0.1837	43.8136	0.1100	150–293	Research mesh already Z-up by (X, −Z, Y); no additional yaw
LY	0.0000	70.4000	0.1760	160–288	(X, −Z, Y); Z minimum removed; yaw +8.5°

Table S4 Effects of boundary decisions on conditional profile distances

Raw means before boundary review; after review excludes the unconfirmed LY eave 9 mean. All other retained observations and settings are the same. Δ is after review minus raw and was calculated before display rounding, so it need not equal the difference of two rounded cells. D_1 and D_2 compare dimensionless width profiles over h = 0–1. These four dependent comparisons involve LY*; the six comparisons among the four main cases are unchanged. D_∞ changes are zero within 10^{-12}. Small nonzero changes use scientific notation.

Pair	Raw D_1	After-review D_1	Δ D_1	Raw D_2	After-review D_2	Δ D_2
CY–LY*	0.1461	0.1457	-3.84×10^{-4}	0.1534	0.1530	-3.93×10^{-4}
CS–LY*	0.1014	0.1011	-3.84×10^{-4}	0.1240	0.1236	-3.99×10^{-4}
CX–LY*	0.0377	0.0373	-3.84×10^{-4}	0.0420	0.0416	-4.62×10^{-4}
QZ–LY*	0.0268	0.0264	-3.84×10^{-4}	0.0303	0.0300	-3.53×10^{-4}

Table S5 Profile distances under direction and width-definition tests

After-review D_1 uses the retained two-direction means. Each direction range spans 8,100 combinations of local horizontal direction, as described in Note 3. Area-equivalent and Cauchy widths use convex hulls and each tower's own first-eave denominator. They have not undergone new architectural boundary review. All D_1 values are dimensionless integrated absolute profile differences over h = 0–1. An asterisk marks a comparison with the LY conditional profile. Ranges are scenario bounds, not confidence intervals.

Pair	After-review D_1	Direction grid range	Area-equivalent D_1	Cauchy D_1
CY–CS	0.0674	0.0623–0.0725	0.0671	0.0666
CY–QZ	0.1400	0.1306–0.1430	0.1356	0.1362
CY–CX	0.1084	0.1053–0.1157	0.1114	0.1120
CY–LY*	0.1457	0.1423–0.1538	0.1466	0.1483
CS–QZ	0.0809	0.0725–0.0865	0.0787	0.0790
CS–CX	0.0738	0.0708–0.0806	0.0756	0.0758
CS–LY*	0.1011	0.0978–0.1082	0.1029	0.1034
QZ–CX	0.0316	0.0201–0.0326	0.0242	0.0242
QZ–LY*	0.0264	0.0250–0.0309	0.0284	0.0281
CX–LY*	0.0373	0.0317–0.0434	0.0352	0.0363

Table S6 Complete direct and residual profile distances

D_1 is the integrated absolute difference; D_2 is the square root of the integrated squared difference; $D\infty$ is the largest absolute difference. All use dimensionless widths normalized by each tower's own first studied mean width and relative heights h = 0–1. Residual distances first subtract each tower's own straight line joining its first and last normalized widths. Six pairs compare the four main cases; four pairs marked with an asterisk include LY conditionally. Note 3 gives the integration rules.

Pair	D_1	D_2	$D\infty$	Residual D_1	Residual D_2	Residual $D\infty$
CY–CS	0.0674	0.0889	0.1884	0.0663	0.0879	0.1879
CY–QZ	0.1400	0.1431	0.2016	0.0492	0.0640	0.1365
CY–CX	0.1084	0.1126	0.1856	0.0304	0.0371	0.0741
CY–LY*	0.1457	0.1530	0.2633	0.0340	0.0406	0.0873
CS–QZ	0.0809	0.0989	0.1965	0.0244	0.0278	0.0519
CS–CX	0.0738	0.0882	0.1805	0.0480	0.0562	0.1170
CS–LY*	0.1011	0.1236	0.2582	0.0495	0.0553	0.1019
QZ–CX	0.0316	0.0347	0.0678	0.0239	0.0296	0.0660
QZ–LY*	0.0264	0.0300	0.0616	0.0251	0.0284	0.0505
CX–LY*	0.0373	0.0416	0.0777	0.0047	0.0062	0.0174

Table S7 Effects of omitting eaves and shifting measurement bands

Baseline D_1 uses measurements retained after review. An omission removes one internal mean while retaining the height limits and first-width denominator. A uniform band shift moves every selected band in a case by the same offset; original relative heights remain fixed and the shifted first width supplies the denominator. n counts numerical scenarios, not buildings or reviewers. Ranges give minimum and maximum D_1 across those scenarios. An asterisk identifies LY conditional comparisons; its eave 9 remains missing.

Pair	Baseline D_1	Omit n	Omission D_1 range	Shift n	Shift D_1 range
CY–CS	0.0674	22	0.0611–0.0689	25	0.0544–0.0710
CY–LY*	0.1457	21	0.1394–0.1483	25	0.1319–0.1528
CY–QZ	0.1400	16	0.1337–0.1421	25	0.1200–0.1427
CY–CX	0.1084	22	0.1021–0.1123	25	0.0960–0.1146
CS–LY*	0.1011	21	0.0984–0.1021	25	0.0994–0.1178
CS–QZ	0.0809	16	0.0784–0.0819	25	0.0695–0.0977
CS–CX	0.0738	22	0.0698–0.0748	25	0.0709–0.0883
LY–QZ*	0.0264	15	0.0238–0.0285	25	0.0263–0.0346
LY–CX*	0.0373	21	0.0365–0.0399	25	0.0263–0.0482
QZ–CX	0.0316	16	0.0277–0.0338	25	0.0164–0.0382

Table S8 Complete sensitivity results for the two highlighted comparisons

Δw is the first case's normalized width minus the second's at $h = 0.25$, measured from the first to last studied eaves. Each case uses its own first-eave denominator. n is the number of scenarios; the final column counts those retaining the baseline sign. First-reference tests change only the denominator and restore $w(0) = 1$. Thickness tests use 0.5, 1 or 2 times the original band at unchanged centers. The sign counts are numerical sensitivity results, not reviewer agreement or statistical confidence.

Pair	Diagnostic	n	D_1 range	Signed Δw at $h = 0.25$	Sign retained
CY–CS	One mean omitted	22	0.0611–0.0689	-0.1407 to -0.1345	22/22
CY–CS	Coherent shift	25	0.0544–0.0710	-0.1421 to -0.1144	25/25
CY–CS	First width only	25	0.0641–0.0787	-0.1542 to -0.1331	25/25
QZ–CX	One mean omitted	16	0.0277–0.0338	0.0414 to 0.0516	16/16
QZ–CX	Coherent shift	25	0.0164–0.0382	0.0290 to 0.0546	25/25
QZ–CX	First width only	25	0.0105–0.0546	0.0140 to 0.0724	25/25
CY–CS	Band thickness	9	0.0658–0.0681	-0.1393 to -0.1350	9/9
QZ–CX	Band thickness	9	0.0273–0.0327	0.0407 to 0.0453	9/9

Table S9 Directional width loss under uniform mesh sampling

All rows refer to Chongxing Temple West (CX). At each density, median and maximum summarize the ten seeds for the stated eave and axis. Width loss is 100 × (1 − sampled width/full-mesh width), using the same band and direction, and is expressed as a percentage. The two sample sizes are 150,000 and 500,000 points. All 520 records met the minimum of ten sampled points per band. These losses describe representation of the fixed mesh, not error relative to independent field dimensions.

Eave	Axis	150,000 points Median loss (%)	150,000 points Maximum loss (%)	500,000 points Median loss (%)	500,000 points Maximum loss (%)
1	X′	1.0838	2.5181	0.4061	0.6401
1	Y′	0.9375	1.9667	0.4210	1.1192
2	X′	0.6969	1.0317	0.2804	0.4738
2	Y′	1.1093	1.9431	0.3380	0.9556
3	X′	0.6042	1.3913	0.4085	0.6996
3	Y′	1.3071	1.6879	0.4988	1.0184
4	X′	1.2054	1.7567	0.3309	1.0642
4	Y′	1.0037	1.3827	0.4355	0.9025
5	X′	0.7970	1.5805	0.6479	0.9816
5	Y′	0.8003	1.2993	0.5198	0.8325
6	X′	1.0008	1.4947	0.5009	1.0127
6	Y′	0.8001	3.0295	0.4673	0.9825
7	X′	1.1226	1.7120	0.9414	1.3648
7	Y′	0.7460	1.5211	0.4569	0.9062
8	X′	1.3412	1.6746	0.6231	1.1853
8	Y′	1.3514	2.2081	0.4887	1.1194
9	X′	1.9554	2.4996	0.6195	1.5578
9	Y′	0.8649	2.3630	0.6030	1.1363
10	X′	0.8627	1.8295	0.4446	1.2271
10	Y′	1.5273	2.5383	0.7166	1.1375
11	X′	1.7332	2.7533	0.7796	1.7060
11	Y′	1.6324	2.2357	1.0157	1.6526
12	X′	1.1192	2.5396	0.6615	1.3542
12	Y′	1.3038	2.6612	0.4863	1.2680
13	X′	1.2629	2.2283	0.7103	1.5530
13	Y′	1.1562	1.9026	0.4519	0.9423

Table S10 Recorded independent review and targeted follow-up

R01–R12 identify reviewed directions; R1 and R2 identify reviewers. R1 responses were relayed by the author on 12 October 2026. R2 responses were recorded as received on that date, but the actual review date and confidence were not supplied. R1 confidence uses a 1–5 scale. Not requested means there was no R2 assessment, not that R2 agreed. Current use gives the boundary state and analysis in which the measurement is retained. Answers and confidence do not automatically change that use. In particular, R07 remains excluded and R12 remains conditional; Note 2 explains why.

ID	Reviewed direction	R1 answer	R1 confidence	R2 answer	Current use
R01	CX E13 X′	yes	5	Not requested	A; main comparison
R02	CX E1 Y′	yes	5	Not requested	A; main comparison
R03	QZ E7 Y′	yes	5	Not requested	A; main comparison
R04	CS E1 X′	yes	5	Not requested	A; main comparison
R05	LY E9 Y′	yes	5	Not requested	A; LY conditional analysis
R06	LY E6 X′	yes	5	Not requested	A; LY conditional analysis
R07	LY E9 X′	yes	3	unclear	Not accepted; no two-direction mean
R08	CS E13 Y′	yes	5	Not requested	A; main comparison
R09	CY E2 X′	yes	5	Not requested	A; main comparison
R10	QZ E1 X′	yes	5	Not requested	A; main comparison
R11	CY E2 Y′	yes	5	Not requested	A; main comparison
R12	LY E10 X′	yes	3	yes; retain point	B; LY conditional analysis

Table S11 Unresolved evidence for 15 conditional Liaoyang directions

All directions belong to LY and remain B, meaning retained for conditional analysis with unresolved evidence. Widths are local model units. The final column states the remaining component or photograph-to-model question, even where an earlier affirmative response is recorded. No verified replacement coordinate was adopted. LY eave 9 X′ is separately unaccepted and is not one of these 15 directions. R12 refers to eave 10 X′, not eave 13 X′.

Direction	Retained width	State	Unresolved correspondence
E2 X′	18.3631	B	Both ends lie near corner junctions; ornament versus ordinary tile-edge correspondence is unresolved.
E2 Y′	18.4036	B	Negative end is near ornament; positive end has branches and low illumination.
E4 X′	17.7268	B	Negative end is near ornament; positive corner extension lacks independent component correspondence.
E4 Y′	17.6215	B	Both ends approach corner ornament; positive end is dark.
E7 X′	16.8215	B	Negative end is near the corner; positive end is near a bell suspension. Markers alone do not establish membership.
E7 Y′	16.8354	B	Negative ornament and precise positive corner boundary lack independent correspondence.
E8 X′	16.4516	B	Both endpoints are near tile-edge and corner-decoration junctions.
E8 Y′	16.4693	B	Negative end is near the corner; positive end is dark with branch background.
E10 X′	15.8412	B	Author disputed the original photo marker. The proposed image point was not triangulated; an alternative projection falls below the eave.
E10 Y′	15.8727	B	Earlier informed affirmation is not independent review; exact correspondence remains limited by block registration.
E11 X′	15.5139	B	Dark positive photo and sparse local mesh do not independently fix the visible tile terminal.
E11 Y′	15.5770	B	Negative end is near the corner and positive end is poorly illuminated.
E12 X′	15.1114	B	Dark positive end close to the corner; extremal component remains independently unresolved.
E12 Y′	15.1827	B	Positive point neighbors ornament; continuous mesh alone cannot exclude an attachment.
E13 X′	14.9978	B	Positive projection lies near roof and vegetation; existing affirmation lacks an independently fixed tile-edge coordinate.

Table S12 Working-mesh identities

Full SHA256 strings retain all digits; line breaks are for layout only and must be removed when checking them. CX source OBJ SHA256 is 0ef5a10f99e7026a56e631482e8a58d5525237227c24965356c74303ddf69330. Its transformed vertex and triangle arrays correspond to the working PLY. Hashes establish file identity only. The case abbreviations follow Note 1. Vertex and triangle counts describe the working files listed here; they are not independent quality or accuracy measures.

Case	Format	Vertices	Triangles	SHA256
CY	OBJ	8,254,489	2,751,834	8c4db51af48d08f97bb5b434c0890df7 121ec3c7fecda8e3a29988aade9e4d87
CS	Cropped OBJ	8,157,054	2,719,333	8cade4cb1c3b1bba422a936f90873aa5 69f8e3354f0d73cf19c7878bcba51e8b
QZ	Research PLY	782,876	1,554,922	24f1f25ab632a3bd8eb84460dcb953fb 7f5152b3f72b59e02809a2cee05871c4
CX	Research PLY	2,125,252	4,164,776	5c3846f439ac1b4ac1485bdcc1124743 0bc31a00104c6c055342ae2cad26d2a8
LY	OBJ	14,793,546	4,934,416	d4365e6be2fc8c49cce3e36d1e24ac5c 686b1f1fc1e5b2238a03c1b37ab3ad06

Table S13 Algorithm S1 for comparison with recorded boundary decisions

Algorithm S1 summarizes the existing calculation; equation numbers refer to the main article. The boundary target, coordinate frame and evidence are specific to each building. Confirmed measurements enter the main comparison, retained unresolved measurements enter only the conditional analysis, and unaccepted directions leave the two-direction mean missing. The algorithm introduces no new observations or inferred eaves.

Operation	Specification
1 Define and record the target	Record the chosen eave boundary, upward numbering, mesh identity, environment mask, coordinate transform, 400-band grid and first/last study-eave centers.
2 Clip each measurement band	Intersect each source triangle with $z_lower \le z \le z_upper$. Retain in-band vertices and edge-plane intersections. Apply the frozen environment mask; do not repair holes or mirror geometry.
3 Extract directional widths	$Wx = \max(x') - \min(x')$; $Wy = \max(y') - \min(y')$. Retain one signed coordinate at each extremum and its source correspondence. Width is a projection, not the Euclidean distance between the selected coordinates.
4 Review the boundaries	Review both signed points for target membership, local continuity, tier and boundary definition. Record A, conditional B or unadopted status. A mean requires two retained directions. Preserve historical inference separately.
5 Normalize retained observations	For retained pairs, $Wi = (Wx + Wy)/2$; $hi = (center\ \ i - center\ \ first)/(center\ \ last - center\ \ first)$; $wi = Wi/Wfirst$. Retain the original limits in omission scenarios. Missing Wi stays missing.
6 Interpolate profiles and calculate departures	Join retained (hi, wi) with straight segments. Label intervals across missing means as interpolation. Use $c(h) = 1 + (wlast - 1)h$ and $r(h) = w(h) - c(h)$. Integrate signed residual area without replacing it by absolute area.
7 Compare profiles at combined heights	Merge both cases' h knots. Interpolate each profile there. On each interval use the exact absolute or squared linear-difference integrals specified after Eq. (3); $D\infty$ is the greatest absolute knot difference. Repeat for residuals.
8 Test measurement choices	Omit each internal paired mean once; apply five coherent slab shifts with scenario-specific first widths; test first-reference-only and thickness scenarios; compare hull-width definitions and independent 0–89° direction grids. Keep unresolved measurements missing and report prescribed ranges.

Supplementary figures

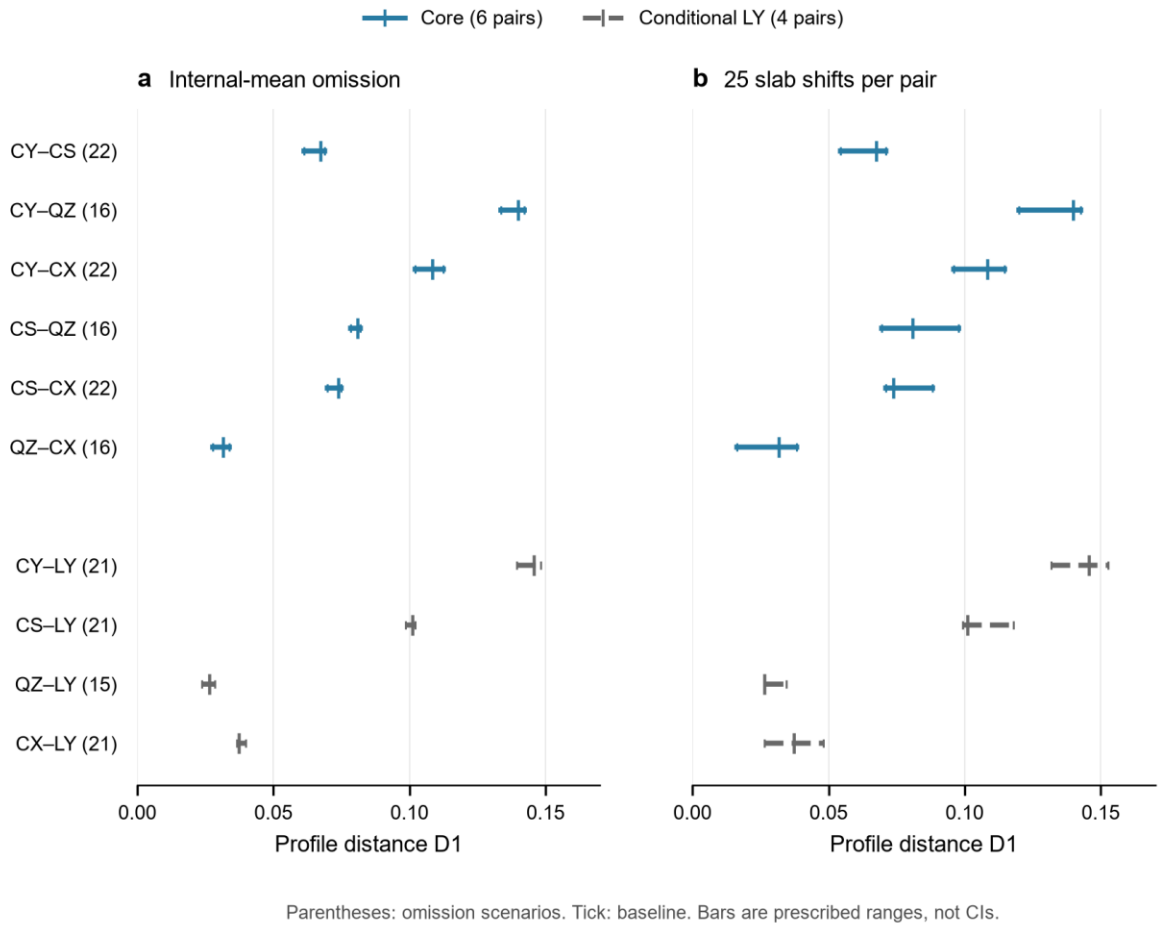


Figure S1 Sensitivity of profile distances to eave omissions and measurement-band shifts. CY, CS, QZ, CX and LY denote Chaoyang North, Chongshou Temple, Qingzhou White, Chongxing Temple West and Liaoyang White. D_1 integrates the absolute difference between dimensionless width profiles; each width is divided by its tower's first studied mean width, and h spans the first to last studied eaves. Vertical ticks mark the baseline D_1; bars span numerical scenarios rather than confidence intervals. (a) Removing one internal mean gives 22 scenarios for CY–CS and 16 for QZ–CX; counts for all ten pairs total 192 affected comparisons. (b) Five band offsets per case give 25 combinations per pair and 250 overall. Original relative heights are retained; each shifted profile uses its shifted first-width denominator. The six main-case pairs precede four LY conditional pairs. Core in the image denotes the four main cases.

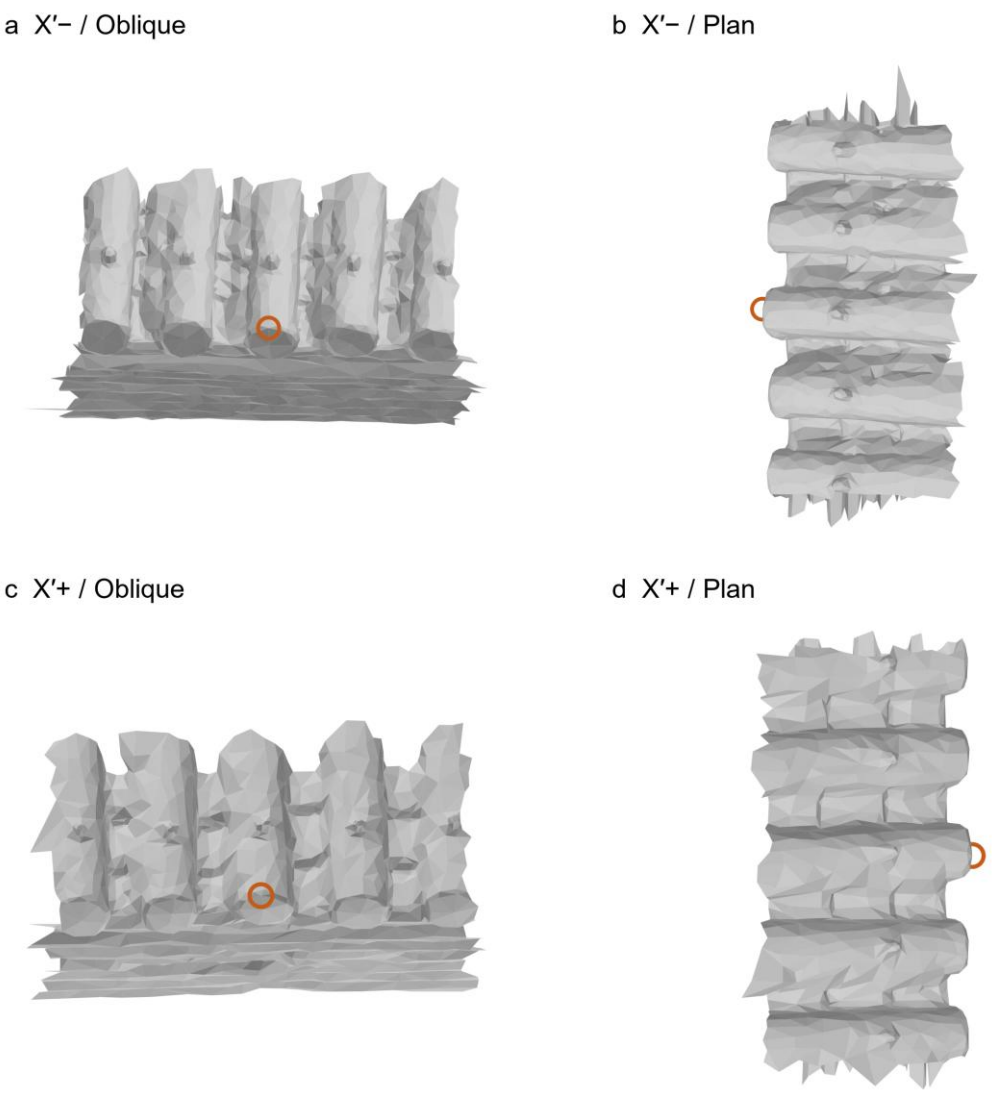


Figure S2 Review of the exact Chaoyang North eave 2 X′ endpoints. (a,b) Original-triangle views around the negative endpoint, shown obliquely and in plan. (c,d) Corresponding views around the positive endpoint. Circles locate recorded coordinates and do not certify the boundary. On 10 October 2026 the author confirmed that both points belong to the same continuous tile-terminal edge and retained them. The earlier AI-assisted inspection is historical context rather than an independent human assessment. No geometry was repaired. The earlier change from 23° to 22.5° changed the measurement direction and was not a correction from the matched boundary review. Offsets are local model units. CY denotes Chaoyang North; E2 denotes eave 2; X′− and X′+ identify the negative and positive endpoints.